An experimental investogation of mode-I interlaminar fracture of composite pipes

1st Fares Mohammed Laid REKBI, 2nd Mabrouk HECINI, 3rd Abdelhak KHECHAI

1st Mechanical Engineering Laboratory, University of Biskra, Algeria.
2nd Mechanical Engineering Laboratory, University of Biskra, Algeria.
3rd Civil Engineering Laboratory, University of Biskra, Algeria.

Corresponding Author: faresgmb@gmail.com

***Abstract*— A common industrial production process for composites is filament winding, widely used for the production of axially symmetric components. In these composite components, delamination is a predominant failure mechanism. The current work focused on investigating the possibilities of determining the effect of the initial crack on the interlaminar fracture toughness G_{IC} and the compliance *C*, which enable the investigation of resistance curve (R-curve) behavior for mode I delamination growth. For this purpose, DCB specimens with stacking sequence of $[\pm 50]_6$ and initial crack length of a_0=33, 37, 59 and 70 mm are manufactured as a composite pipe by the filament winding process. In order to evaluate the critical energy release rate in mode I, fracture tests are conducted on these specimens. Results show that the magnitudes of initiation delamination toughness ($G_{IC\text{-}init}$) are constant in a range of the initial crack length to the DCB specimen $33 \leqslant a_0 \leqslant 70$ mm. Finally, $G_{IC\text{-}init}$ measurements are compared with those from the Finite Element (FE) models. The numerical results from the FE models are in good agreement with the experimental results.**

Keywords— Critical energy release rate, propagation energy release rate, filament wound composite, DCB specimen, R-curve

I. Introduction

The use of composite pipes made by filament winding is, in fact, expected to increase in the future and will include crude oil transportation. This increasing use has motivated researchers to understand their failure mechanism. Under functioning conditions, a real structure is always submitted to undesired loading events. All these events can generate defects, and their effect must be determined to guarantee the safe operation of the structure [1]. These defects may be caused from manufacturing imperfections, accumulation of voids during the production and low speed impact loading during service, cracks produced by fatigue or low velocity impact, stress concentration near joints and free edges, or due to high inter-laminar stresses [2, 3]. The delamination in composites pipe is even more complex compared to plane structures and very few studies have been conducted on the interlaminar fracture of filament wound composites [4-6].

For axially symmetric components, two different sample geometries can be obtained: the samples can be cut in the axial (longitudinal) or hoop (transverse) direction. In the literature, there are different examples of the use of both types of samples: Ozdil at al. [5, 6] and Davies et al. [4] tested samples cut in the longitudinal direction (direction parallel to the cylinder axis), while Lauke et al. [7, 8] tested samples cut in the transverse direction. The longitudinal samples presented a curved section/crack front but with a straight crack propagation path [2]. In their work, Ozdil at al. [5] evaluated the interlaminar fracture toughness G_{IC} and the compliance *C* for flat and curved double cantilever beam (DCB) with internal curve *R*=80 mm. The results show that the influence of curvature on *C* and G_{IC} is small for the range of curvatures examined and decreases with laminate thickness. Davies et al. [4] also evaluated the G_{IC} value on both filament wounded plates (almost unidirectional) and tubes (with three different winding angles). The results showed similar G_{IC} values for the different tests. Based on these results, DCB test is usually used for studying mode I delamination. Andersons and König [9] presented a comprehensive review on the published experimental research concerning delamination onset and growth in laminated composites under various mode loadings.

The interlaminar fracture of multidirectional composites has already received considerable attention and more recent works on this problem were given in [8, 11-12]. In all the above-mentioned research, G_{IC} values at initiation and especially propagation is reported for a definite crack length and thickness to conduct definite goals. However, the delamination behavior or *R*-curve behavior of filament wound composite pipes was not fully characterized in detail.

The current work focused on investigating the possibilities of determining the effect of the initial crack on the interlaminar fracture toughness G_{IC} and the compliance *C*, which enable the investigation of *R*-curve behavior for mode I delamination growth. In this work, we use flat specimens in view of the simplicity of testing and data reduction. Different longitudinal DCB test were machined from a pipe. In each *R*-curve, two parameters, i.e., initiation and steady state propagation toughness are carefully investigated. In the next section, material and specimen preparation procedures and delamination tests are explained. Then, data reduction methods for calculation the interlaminar fracture toughness and *R*-curve behavior of DCB specimens are introduced. The experimental results are presented and discussed in detail followed by the FE models to validate the experimental results. Finally, conclusions are presented in the last section.

II. Experimental

A. *Material and specimen preparation*

In this section, the main objective is to give the essential steps of the experimental study on real produced filament wound composite pipe. The testing specimens were taken from real filament wound pipe manufactured using glass fiber reinforcement impregnated with catalyzed polyester resin with fiber volume fraction equal to 75%. The glass fiber reinforcements are wound with a slight tension on a cylindrical mandrel. The DCB test specimens were prepared according to standard ASTM D5528-94a [13]. The specimens used were 200 mm length and 25 mm width and the thickness of the DCB specimen was 5 ± 0.15 mm. The initial crack lengths were a_0 = 33, 37, 59 and 70 ± 0.2 mm (Fig.1 a). The specimens used in this work consisted of plies having ±50° orientation, with the average of 75% fibre volume fraction. The laminates contain six layers [50/-50/50/-50/50/-50] to have the Mylar film placed in the mid-plane to act as a crack starter. The measured mechanical properties of each layer E_1=54800 (MPa), E_2=E_3=11294 (MPa), G_{12}=G_{13}=5428.6 (MPa), G_{23}=5292.6 (MPa), v_{12}= v_{13}=0.32, v_{23}=0.06. The load (P) is transmitted by the pins that allow free rotation of the piano hinge during the test to avoid moment at the loading point (Fig.1 a).

Four identical test specimens were produced for each specimen design. The DCB test setup is shown in (Fig. 1 b).

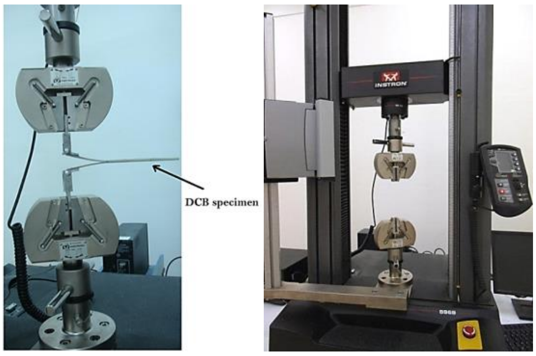

(a)

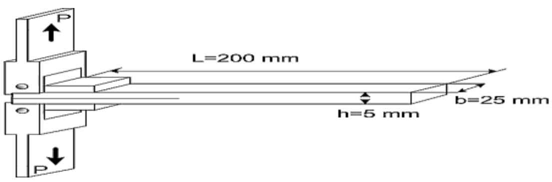

(b)

Fig.1: Experimental setup for DCB testing.

A universal testing machine (INSTRON-5969) was used to conduct the tests on the laminate specimens (see Fig. 1 a). The testing machine is connected with a computer to record the stress/strain curve during the tensile process.

III. THEORETICAL

A. Calculation of interlaminar fracture toughness G_{IC}

The delamination strength is evaluated by the critical energy release rate G_{IC} corresponding to the initiation of the crack. The mode I critical energy release rate can be experimentally determined by several methods mentioned in [13] namely: modified beam theory MBT method, compliance calibration CC method and modified compliance calibration MCC method. The modified beam theory MBT is one of the most frequently used methods for characterizing the fracture toughness of DCB specimens. The following formula was recommended by ASTM D-5528-94a [13] for calculation the G_{IC} based on the CC method:

$$G_{IC} = \frac{nP_c\delta}{2ab}$$

Where b represents the specimen width and P_c is the critical load corresponding to the initiation of the crack. The critical load P_c is defined either by PNL (end of the linear part of the curve) either by $P_{5\%}$ (charge corresponding to stiffness drop of 5%). According to CC method, compliance is also given as a function of two intrinsic constants of the material h' and n using the formula $C=a^n/h'$ where h' and n are the intrinsic parameters of the material. The value represents the slope of the log(C)/log(a) plot. In the next section, mode I interlaminar fracture toughness is characterized by these two methods.

B. R-curve of DCB specimens

R-curve describes the evolution of resistance to delamination in accordance with the increase of the crack after the initiation point of delamination. In the case of DCB specimen's type, the length of the crack was determined, in an effective way, from the law of compliance based on CC method:

$$a_{eff} = \sqrt[n]{Ch'}$$

Where C is measured in the part after the initiation of crack propagation. Then the corresponding resistance is determined by the following relationship:

$$G_{IP} = \frac{nP_c^2}{2bh'} a_{eff}^{\,n-1}$$

IV. RESULTS AND DISCUSSION

Fracture analysis has been carried out on the double cantilever beam specimens made from real filament wound composite pipe [±50°]$_6$ with three different crack lengths. Crack growth in the specimens occurred from the delamination starter, located between the +50° and the -50° plies in the center of the beams.

In order to compare the typical curves found for different laminated DCB specimens, with various initial crack lengths, the load–crack growth are plotted in Fig.2. As depicted in this figure, the behavior is essentially linear up to the NL points (the point of the deviation from the linearity part of the curve). Following the linear part, by increasing the delamination length, bearing load capacity of the specimens increased up to a highest load due to the fiber bridging phenomenon. After this part, load-displacement curves have nonlinear behavior and the stiffness of the composites pipes specimens changes. Consequently the slopes of (P-δ) curves decrease. It has been observed that the critical load of the DCB specimen with crack length a_0=70 mm is lower than those of the other specimens. On the other hand, in all the DCB specimens, mild ''stick–slip'' instabilities phenomenon is observed after the delamination growth. This phenomenon is probably associated with the periodical transverse cracking and crack jumping between two adjacent +50°/-50° interfaces. Ozdil and Carlsson [10] and Shokrieh et al. [14] have also pointed out this phenomenon in their research.

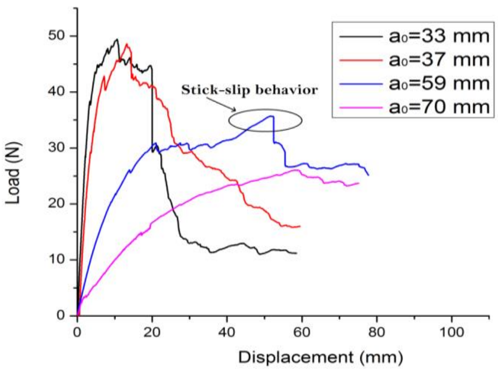

Fig.2: Load–displacement curves of the DCB specimens with various initial crack lengths.

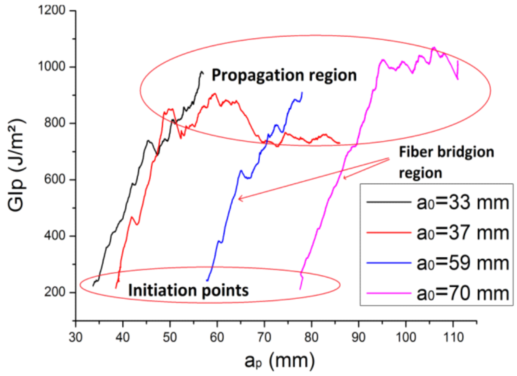

Fig.3: Load–displacement curves of the DCB specimens with various initial crack lengths.

A. *Initiation delamination toughness, $G_{IC\text{-}init}$*

Table 1 presents the critical load and displacement at the NL point of the load-displacement curve as well as the compliance at the delamination onset for different DCB specimens with various initial crack lengths. These values are used to determine the initiation energy release rate GIC-init based on the two MBT and CC methods. It can be observed that the GIC-init values are approximately constant for all the specimens despite the changing in the initial crack length (33≤ a0 ≤70 mm).This indicates that the initiation resistance of delamination GIC-init a constant intrinsic characteristic or a material property of composite materials; and that is independent of the initial crack length and specimen size and geometry. On the other hand, one can see that the GIC-init values based on the MBT method are slightly less than that of obtained by the CC method.

TABLE I. RESULTS OF COMPLIANCE AND INITIATION DELAMINATION TOUGHNESS VALUES.

a_0 (mm)	Critical values at NL		Compliance $\mu m / N$	$G_{IC-init}$ J / m^2	
	Pc (N)	Disp		CC	MBT
33	37.474	3.161	84.335	227.530	194.745
37	31.761	4.101	129.100	223.147	192.959
59	21.676	10.142	467.840	236.212	211.064
70	4.411	6.170	1122.053	211.051	190.025

B. *Propagation delamination toughness, $G_{IC\text{-}prop}$*

In compliance curves of DCB specimens, it is seen that after the initiation of the delamination propagation the compliance is continuously increased with the delamination length. Fig. 3 shows the interlaminar fracture toughness versus delamination growth. The *R*-curves were obtained from the experimental *P-δ* curves considering the CC method. According to the *R*-curves illustrated in Fig. 3, a similar behavior was shown for all the DCB specimens, i.e., increasing behavior with the same slope. This curve begins from the initiation energy release rate and rises by increasing the crack growth. It is interesting to note that this is due to the interaction between the interlaminar crack and the unbroken fibers left behind the crack front while the crack switches from one fiber–matrix interface to another as it propagates. It is so-called named as fiber bridging phenomenon [14]. After passing the transient zone, namely the fiber bridging region, the value of fracture toughness reaches to a steady-state value. Fiber bridging has been reported in Refs. [15-16].

C. *Model validation*

In this section, our main goal is to compare the numerical results obtained using finite element software with those found previously in the experimental section. The geometric model for the delamination problem in the DCB specimens is a beam with a total length of 200 mm, 25 mm width, and 5 mm thickness as a result of the *t* = 0,84 mm ply thickness. The initial crack starts at a distance of 33 to 70 mm from the edge.

Because the experimental testing specimens were taken from a real filament wound pipe, the present finite element model was modeling with an internal diameter of *R*=250 mm. Commercial finite element FE software, ABAQUS®, was used to perform all simulations. FE models were constructed using 3D eight-node brick elements (C3D8R). Fig. 4 represents schematically the model loading and boundary conditions. (Fig. 4 a) shows a typical FE mesh. In present study, each specimen was modeled by reduced integration (C3D8R) elements with one integration point per element. The elastic properties of each ply are given in the experimental. One end of the beam is fixed, and the other end is loaded, at the top and bottom nodes of the edges, with an external force with the same magnitude but opposite direction as shown in (Fig. 4 b).The corresponding applied load is the experimental critical load *P*.

A convergence study of the 3D model is initially performed. The final model includes 2355 nodes and 1680 elements. In actual tests, GIC calculated from the critical load P and numerical displacements δ recorded for specified crack length a0 is presented in Table 2. After simulation the numerical and experimental GIC were compared.

TABLE II. RESULTS OF COMPLIANCE AND INITIATION DELAMINATION TOUGHNESS VALUES.

a_0 (mm)	Critical values at NL		$G_{IC-init}$ J / m^2		Numerical Results	
	Pc (N)	Disp. (mm)	CC method	MPT method	Disp. (mm)	$G_{IC-init}$ J / m^2
33	37.474	3.161	227.530	194.745	3.836	276.227
37	31.761	4.101	223.147	192.959	4.487	244.242
59	21.676	10.142	236.212	211.064	11.620	270.710
70	14.411	16.170	211.051	190.025	12.850	167.753

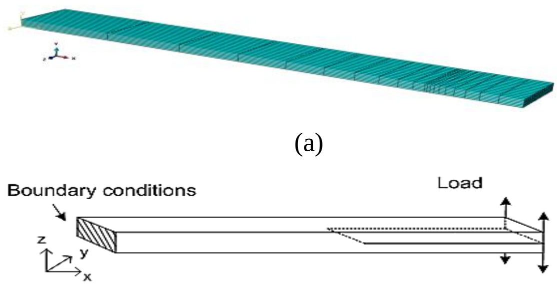

(a)

(b)

Fig.4: Finite element mesh, loading and boundary condition. (a) Mesh model. (b) Loading and boundary condition.

The deformed shapes for the DCB FE model are shown in Fig. 5. The DCB FE model is shown when the crack growth is maximum.

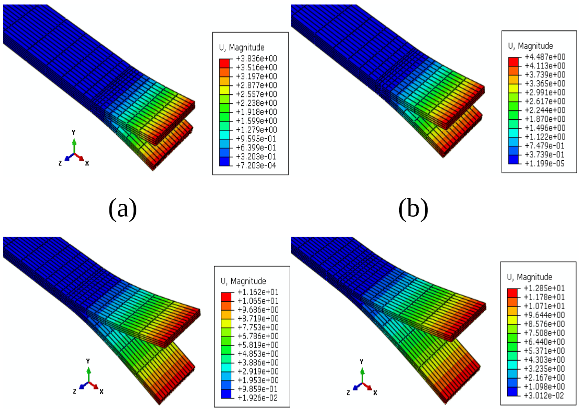

(a) (b)

(c) (d)

Fig.5: The deformed shapes for the DCB FE model.

As it can be seen in Table 2 that the numerical displacement δ value is very close to the experimental one. In addition, the G_{IC} values for all numerical models are in good agreement with the experimental results, thus validating the experimental results.

V. CONCLUSION

The main goal of this study is to investigate the effects of delamination on composite pipes behavior. In these composite components, delamination is a predominant failure mechanism. Our study focused to determine the effect of the initial crack and fiber bridging length on the fracture behavior of DCB specimens during the initiation and propagation of delamination. The tested samples were cut in the longitudinal direction from the composite pipe. Afterwards, the delamination tests based on ASTM standard were conducted on DCB specimens and the energy release rate was characterized based on the MBT and CC methods. In the present research, the mode I *R*-curve behavior of the composite pipe with different crack lengths are investigated. For this purpose, DCB specimens with stacking sequence of $[\pm 50]_6$ and initial crack length of a_0=33, 37, 59 and 70 mm are manufactured as a composite pipe by the filament winding process. In order to evaluate the critical energy release rate in mode I, fracture tests are conducted on these specimens. Results show that the magnitudes of initiation delamination toughness ($G_{IC\text{-}init}$) are constant in a range of the initial crack length to the DCB specimen $33 \leqslant a_0 \leqslant 70$ mm. The results indicate that the fiber bridging has significant effect on the G_{IC} and causes a large fracture toughness value. Finally, $G_{IC\text{-}init}$ measurements are compared with those from the FE models. The numerical results from the FE models are in good agreement with the experimental results.

REFERENCES

[1] Buarque, E. and J. d'Almeida, The effect of cylindrical defects on the tensile strength of glass fiber/vinyl-ester matrix reinforced composite pipes. Composite Structures. 79(2): p. 270-279, 2007.

[2] Perillo, G. and A. Echtermeyer, Evaluation of mode I interlaminar fracture toughness of filament-wound gfre composite pipe. 15th European conference on composite materials, ECCM, Venice, Italy. P. 24-28, 2012.

[3] Kormaníková, E. Delamination of Laminate Plates. in Advanced Materials Research. Trans Tech Publ. 2014.

[4] Davies, P. and F. Rannou, The effect of defects in tubes: Part 1. Mode I delamination resistance. Applied Composite Materials. 1(5): p. 333-349, 1994.

[5] Ozdil, F. and L. Carlsson, Characterization of mode I delamination growth in glass/epoxy composite cylinders. Journal of Composite Materials. 34(5): p. 398-419, 2000.

[6] Ozdil, F. and L. Carlsson, Characterization of mixed mode delamination growth in glass/epoxy composite cylinders. Journal of Composite Materials. 34(5): p. 420-441, 2000.

[7] Lauke, B. and K. Friedrich, Evaluation of processing parameters of thermoplastic composites fabricated by filament winding. Composites Manufacturing. 4(2): p. 93-101, 1993.

[8] Beckert, W., B. Lauke, and K. Friedrich, Delamination toughness computation for curved thermoplastic composites. Applied Composite Materials. 1(5): p. 395-400, 1994.

[9] Andersons, J. and M. König, Dependence of fracture toughness of composite laminates on interface ply orientations and delamination growth direction. Composites Science and Technology. 64(13): p. 2139-2152, 2004.

[10] Ozdil, F. and L. Carlsson, Beam analysis of angle-ply laminate DCB specimens. Composites Science and Technology. 59(2): p. 305-315, 1999.

[11] Huimin, F. and Z. Yongbo, On the distribution of delamination in composite structures and compressive strength prediction for laminates with embedded delaminations. Applied Composite Materials. 18(3): p. 253-269, 2011.

[12] F.M.L. Rekbi, M.Hecini., Etude expérimentale du délaminage en mode I des tubes fabriqués par enroulement filamentaire. Revue des Composites et des Matériaux Avancés. 25(3-4): p. 373-384, 2015.

[13] AC09036782, A., Standard test method for mode I interlaminar fracture toughness of unidirectional fiber-reinforced polymer matrix composites: ASTM Internat, 2007.

[14] Shokrieh, M., M. Heidari-Rarani, and M. Ayatollahi, Delamination R-curve as a material property of unidirectional glass/epoxy composites.Materials & Design. 34: p. 211-218, 2012.

[15] Haugen, D.J., Fracture of skin-stiffener intersections in composite wind turbine blade structures, Montana State University-Bozeman, 1998.

[16] Daelemans, L., et al., Nanofibre bridging as a toughening mechanism in carbon/epoxy composite laminates interleaved with electrospun polyamide nanofibrous veils. Composites Science and Technology. 117: p. 244-256, 2015.